Solar Energy Materials & Solar Cells 107 (2012) 236–247

Contents lists available at SciVerse ScienceDirect

Solar Energy Materials & Solar Cells

journal homepage: www.elsevier.com/locate/solmat

Using stochastic models to determine financial indicators and technical objectives for organic solar cells

Colin Powell *, Yuri Lawryshyn, Timothy Bender

200 College Street, Toronto, ON, Canada M5S 3E5

ARTICLE INFO

Article history:
Received 1 February 2012
Received in revised form
17 June 2012
Accepted 22 June 2012
Available online 19 July 2012

Keywords:
Organic solar cells
Stochastic weather model
Mean-reverting electricity price model
TEEOS

ABSTRACT

Organic photovoltaics (PVs) are a rapidly emerging technology that has the potential to provide low-cost power for many different applications. The TEEOS model had previously been developed to determine various financial indicators for this technology. This paper modifies TEEOS in order to better analyze the effects of variability in the inputs. This modified TEEOS incorporates a mean-reverting jump diffusion model to simulate synthetic electricity price and a modified rainfall occurrence model to simulate a weather series. As well, the external quantum efficiency (EQE) is used as an input in order to gain insight on using low band gap polymers or enhancing the existing EQE. The power production NPV of three example cells, a Si-based solar cell, dye-sensitized solar cell (DSSC) and an organic solar cell (OSC), are first examined using a 25-year time period where the DSSC and OSC have to be replaced five times due to low lifetimes. The DSSC and OSC are also compared using five years of actual data using a five-year horizon. The sensitivity analysis looks specifically at inherent increases in the electricity price, the correlation of electricity prices and weather, modeling electricity without jumps, as well as enhancing and expanding the EQE. The best option for increasing the economic feasbility for the OSCs is expanding the EQE, that is, reducing the band gap of the polymers used. A break-even target of $\$45/m^2$ for the OSC is stated, which is on the low range of current cost estimates; this break-even-target would increase for locales closer to the equator.

1. Introduction

Organic photovoltaics (OPVs), made from plastics and other organic materials, are a key energy technology that can be used to open up new markets and applications for photovoltaics (PVs) [1,2]. OPVs have two main advantages over traditional PV technologies: (1) they have the potential to be inexpensive and (2) they are easy to manufacture [3]. However, the current technology is still quite expensive and cost-effective production methods are still being investigated.

The main factors affecting the economics of grid-connected PV-electric projects are location, local weather conditions, local electricity prices and manufacturing and equipment costs. Site location and local weather conditions determine the amount of sunlight the PV array can convert into usable energy. Local electricity prices determine the amount of money an owner of a PV array avoids paying to an electricity provider. The cost of manufacturing OPVs has only recently been discussed [1,4–8] and is still quite expensive, but there is great potential for lowering costs by using lower-cost labour, increasing throughput, and reducing material costs.

Some progress in the technology development has been made. OPVs have been tested as a source of electricity for lighting individual spaces in African homes [5]. They have been transported long distances to test durability and performance [9] and tested outdoors to measure degradation [7]. These demonstrations provide the basis for determining the economic feasibility of OPVs in the real world. But in the absence of larger pilot demonstrations of OPVs, economic models must be used to estimate the financial viability of the technology.

A number of studies exist concerning the economic feasibility of PV in niche applications, such as hybrid diesel/PV or solar thermal systems [10,11], PV combined with demand-side management of electricity [12], and grid-connected PV systems in various locations [13–15]. However, these studies cannot be used to test sensitivities in variables such as volatility in electricity prices, material price fluctuations, and most importantly, enhancing or expanding the incident spectrum of solar materials in order to gauge the economic feasibility of technological choices. Energy and economic software models, such as RETScreen [16], have the ability to evaluate renewable energy applications using different locations, but do not yet include the specificity needed for evaluating OPVs. Estimates of the economic feasibility of OPVs

* Corresponding author. Tel.: +1 416 978 6924; fax: +1 416 978 8605.
E-mail addresses: colin.powell@utoronto.ca (C. Powell), yuri.lawryshyn@utoronto.ca (Y. Lawryshyn), im.bender@utoronto.ca (T. Bender).

0927-0248/$ - see front matter © 2012 Elsevier B.V. All rights reserved.
http://dx.doi.org/10.1016/j.solmat.2012.06.038

have been calculated by Kalowekamo and Baker [6] and Azzopardi et al. [2] in terms of a price per kWh or per peak watt, but these do not account for the avoided cost of electricity. Azzopardi et al. [2], however, did note some specific technical objectives that are key to the success of OPVs, such as 7% efficiency and a 5 year lifetime. As well, the authors of the current work have previously developed a model called TEEOS (Technical and Economic Evaluator for Organic Solar), which can determine financial indicators for OPV using historical electricity price and weather data, and includes enough flexibility to incorporate material price fluctuations and varying band gaps [17]. TEEOS does not, however, allow for performing complex sensitivity analyses, such as with electricity price fluctuations and weather variation. The full description of TEEOS is available in Powell et al. [17] and will not be detailed here, however a correction is made to the overall method. One particular advantage of the TEEOS model in [17] is the ability to test the economic feasibility of incorporating materials that increase the external quantum efficiency (EQE) of existing OPVs or lowering the band gap of specific OPVs. The enhancement of the incident spectrum using various production techniques and the expansion of the incident spectrum using other low bandgap polymers have been discussed widely [49–55], but this discussion has been strictly confined to the synthesis and characteriziation of these materials. The economic consequences of changing the incident spectrum, specifically whether or not increasing the EQE of existing OPVs or reducing the band gap, have yet to be discussed.

This paper presents a modified TEEOS model that incorporates stochastic electricity price and weather models in place of only historical data. This modification enhances the current TEEOS model in three ways: (1) a larger quantity of historical electricity price and weather data are used to train a stochastic model in order provide a more realistic simulation of the performance of OPV; (2) the two stochastic models are correlated to examine the relationship between electricity prices and weather conditions and its effect on PV-system feasibility; and most importantly (3) the modified TEEOS model allows for a more robust sensitivity analysis because it has the ability to easily vary parameters such as cell costs, electricity price, and the incident spectrum of the solar material. These factors set this model apart from the original model and others.

The structure of this paper is as follows. First, a review of stochastic electricity price and weather models is provided. Next, a correction is issued to the method of the TEEOS model in [17]. The methodologies for calibrating the chosen stochastic electricity price and chosen weather model are discussed and a novel method for introducing a correlation between the two is presented. Afterwards, the power production and NPV of three PVs (silicon-based, dye-sensitized organic and organic) in Toronto, Canada, are shown in the modified TEEOS model. Finally, the results of a sensitivity analysis are presented; this will include an examination of enhancing the existing incident spectrum and lowering the band gap of organic solar cell (OSC). Technical recommendations are also made from these results.

1.1. Stochastic models

In this section, the two stochastic models used in the modified TEEOS model are introduced. In the previous TEEOS model [17], actual data for electricity prices and weather were used, but only from one year. The stochastic models were implemented here in order to use more data with the same characteristics as the historical data and because the stochastic models allow for more robust sensitivity analysis. The two stochastic models used are an electricity spot price model and a weather condition model.

1.1.1. Electricity price models

Electricity prices are important to the TEEOS model because these costs would be avoided if one were using a grid-connected PV system instead of taking power from the grid. Electricity spot prices (and not fixed rates) are used in this analysis for two main reasons: (1) variables that make up the spot price models can be varied to analyze sensitivity to inputs and (2) it is assumed that spot prices will eventually be used as the price that consumers pay for their electricity, especially in Toronto where time-of-use pricing is now in place.

Stochastic models are typically used to simulate electricity prices over time because electricity prices exhibit specific characteristics such as mean-reversion, jumps, seasonality, and time-varying volatility structures [18–20]. These characteristics are accounted for in a variety of models, typically for daily average electricity prices, but these models provide no indication of the dynamics on a smaller time scale. For example, the daily electricity price model cannot accurately describe a specific hourly mean reversion price level. Indeed, a daily price model assumes that the mean reversion level is the same over the course of the day, but this is not necessarily an accurate assessment of the price dynamics. Other factors must be included to account for hourly price changes in a time series.

Overviews of different wholesale electricity price models were written by Weron [21] and Escribano et al. [22]. Some authors have recognized a gap between daily average models and the hourly-specific models, such as Borenstein et al. [23]. Li and Flynn [24] considered the change in hourly volatility in fourteen electricity markets. Wolak [25] studied the hourly price dynamics of day-ahead markets in a number of jurisdictions. Others used a neural network approach to forecast the electricity price in various markets, while also considering factors such as demand, capacity shortfalls, and outages [26,27]. Huisman et al. [19] modeled hourly electricity prices for day-ahead markets using the idea that these prices do not follow time-series dynamics, but can be described by treating the information set as panel data. The authors showed that hourly electricity prices exhibit specific characteristics, such as hourly mean-reversion levels and rates. Nogales et al. [28] used time series models, in contrast to Huisman et al. [19], to forecast hourly electricity prices using dynamic regression and transfer function models. Cartea and Figueroa [18] used a mean-reverting jump diffusion model to explain the dynamics of spot electricity prices in Wales and England, while Hikspoors and Jaimungal [29] used a similar model to forecast the spot price for oil.

While these are all useful models, in this paper, the mean-reverting jump diffusion model proposed by Cartea and Figueroa [18] and the hourly modeling techniques by Li and Flynn [24] to account for hourly, diurnal, and monthly price dynamics were used. This electricity price model and the techniques used to develop it are discussed later in the paper.

1.1.2. Weather condition models

Location and local weather conditions are important factors in the TEEOS model because they determine the amount of sunlight available to a PV array to convert into electrical energy. In the previous TEEOS model, a cloud modification factor (CMF) was used to determine that the effect specific weather conditions were having on solar radiation, but historical data was only used for one year. This particular one year of data was repeated every year of the lifetime of the cell, so that the weather condition at one hour on one particular day was the same every single year. This was a vast simplification. To improve upon this, a stochastic weather model was used to better reflect changes in hourly weather conditions. A stochastic weather model uses a fixed set

of weather data to create a new set of synthetic weather data that has the same underlying parameters as the fixed set; for example, cloudy or sunny spells or maximum and minimum temperatures.

Wilks and Wilby [30] provided an extensive review of stochastic weather models from simple analyses of runs of consecutive weather conditions to models of precipitation, known as rainfall occurrence models (ROMs). These models have been used extensively in agricultural, ecosystem, and hydrological impact studies in order to provide synthetic weather series based on weather station records and are based on the Markov chain model [30–32]. A Markov chain is a random process in which the information about the future state of a process is only dependent on the current and past states. A first-order ROM, using Markov chain logic, determines the future state of a weather process (that is, raining or not raining) depending only on the *current* weather conditions. An *n*-th order ROM determines the future state of a weather process depending on the current weather conditions and the weather conditions of the past *n*-1 day(s) [30].

The ROM was modified for this paper because information about rainfall is not specifically needed for the TEEOS model. The point of using the ROM is to determine any reduction in typical solar irradiance that may be absorbed by the PV array. The *amount* of rain is not needed. In this paper, if it is raining, it is assumed to be cloudy, which would result in a significant reduction in energy available to the PV array for most OPV technologies. If it is not raining, it is assumed to be *sunny*, which would not result in a reduction in energy available. Thus, the weather conditions used in this paper were cloudy and clear. These assumptions are further discussed and validated in Powell et al. [17].

In this modified TEEOS algorithm, a correlation between the stochastic electricity price and weather model is necessary because it recognizes the effect weather conditions have on electricity prices. While the modeling of electricity prices includes some implicit weather correlation, stochastic electricity prices are often modeled to explicitly account for fluctuations in weather. Rambharat et al. [33] used a different mean reversion level when certain weather events occur. This mean-reversion level for extreme weather events was calibrated using temperature records under the assumption that temperatures outside typical ranges are associated with higher electricity prices. Johnsen [34] used snowmelt periods, hydroreservoir inflow and temperature to incorporate weather conditions into the price of hydroelectricity in Norway. The correlations of weather conditions and electricity prices have not yet been used to directly evaluate the economic feasibility of solar energy; Powell et al. [17] presented the framework for such an analysis and this was used as a guide in this paper.

2. Methodology

The general methodology behind the TEEOS model was first presented in Powell et al. [17] and will be corrected here, as well as in a forthcoming published correction. This section further describes the methodology associated with developing a stochastic electricity price model and stochastic weather model. First, the stochastic models are presented. Then, the parameter estimation methodology is shown and the datasets are verified. Finally, the correlation between the electricity price and weather models is discussed and these models are incorporated into a modified TEEOS algorithm.

2.1. Corrections and modifications to Powell et al. [17]

In Powell et al. [17], the irradiance was integrated over only the incident wavelength spectrum but multiplied by the overall efficiency. This is incorrect: the irradiance should have been integrated over *all* wavelength ranges under AM1.5. This drastically under predicted the amount of power available for the cells and thus under predicted the annual savings achieved by the sample cell. In order to improve upon the ability of the TEEOS model to examine sensitivities, the methodology was further modified here.

To be able to predict the economic feasibility of enhancing or expanding the incident spectrum of a particular OPV, the spectrum must be used as an input in the TEEOS model. In order to do this, the short circuit current, I_{SC}, was used to produce a wavelength-specific overall efficiency, or the amount of usable power from each wavelength with respect to the total incident power at that wavelength. The process is shown below.

Generally, in the literature, the I_{SC} [A m^{-2} nm^{-1}] at each wavelength in the incident spectrum is not provided; instead, the EQE is provided with respect to the incident spectrum. The EQE is defined strictly as the number of electrons that flow out of the cell per second (the current) divided by the number of photons that hit the cell per second (the power) [50]:

$$EQE_\lambda(\%) = \frac{\#\text{electrons}}{\#\text{photons}} \times 100 = \left(\frac{I_{sc}/e}{P_\lambda/hc}\right)\Big|_\lambda \tag{1}$$

where e is the charge on one electron (1.602×10^{-19} C), P [W m^{-2} m^{-1}] is the incident power at each wavelength in this case from AM1.5, λ [m], h is Planck's constant (6.626068×10^{-34} m^2 kg s^{-1}), and c is the speed of light (3.00×10^8 m s^{-1}).

Eq. (1) can be re-arranged to solve for $I_{SC,\lambda}$ and then used to find a total power efficiency at each wavelength, η_λ:

$$\eta_\lambda = \frac{I_{SC,\lambda} V_{OC} CFF}{P_\lambda} \tag{2}$$

$$\eta_\lambda = \left(\frac{e}{hc}\right)(FFCV_{OC})(EQE_\lambda C\lambda) \tag{3}$$

where FF is the fill factor in the OPV material and V_{OC} [V] is the open circuit voltage of the OPV material. This equation assumes the V_{OC} and the FF do not change significantly as the I_{SC} changes: this is reasonable and the assumption has been used previously in Klampaftis et al. [49]. The only factors that are not constant in Eq. (3) are the EQE and the wavelength. This wavelength-specific efficiency allows us to perform sensitivity analyses (that would otherwise require experimental work) involving the use of material(s) to enhance or expand the incident spectrum, which is shown later.

2.2. Electricity prices

2.2.1. Mean-reverting jump diffusion model

The electricity price model used in this study was a mean-reverting jump diffusion model. The model is shown here and is similar to that used by Cartea and Figueroa [18]:

$$dS_t = \kappa_t(\theta_t(1+\gamma_t) - S_t)dt + \sigma_t dZ_t + (J - S_t)dq_t \tag{4}$$

In Eq. (4), S_t [$/MW-h, where MW-h is megawatt-hour] is the electricity price process, κ_t [h^{-1}] is the hourly speed of mean-reversion for a given month, θ_t [$/MW-h] is the hourly mean-reversion level for a given month, γ_t, is the annual escalation factor applied to the mean reversion level to account for increases in electricity prices due to structural changes such as new capacity and transmission lines, σ_t [$/MW-h] is the hourly volatility for a given month, dZ_t is the standard Brownian motion, J [$/MW-h] is the normally-distributed jump size, and dq_t is a Poisson process.

The interpretation of Eq. (4) is as follows. Most of the time, $dq_t = 0$, so the process is simply the mean-reverting diffusion process. At random Poisson-distributed times (determined by the

Poisson parameter, λ) the price, S_t, will jump from the previous value to a different level, based on the level of J.

2.2.2. Parameter estimation

The electricity price spot prices used for parameter estimation in this model were obtained from the Hourly Ontario Energy Price (HOEP) published by the Independent Electricity System Operator (IESO) in Ontario, Canada [35]. The dataset consists of wholesale hourly spot prices between May 1, 2002, at 12:00 am and June 30, 2009, at 11:00 pm. There were 62,784 observations. Over 99.5% of the electricity prices fall within the range of $0.00/MW-h and $200.00/MW-h. Table 1 includes the electricity price summary statistics for the dataset. The parameters from Eq. (4) were determined using methods described in Cartea and Figeuroa [18] and Clewlow and Strickland [36] and will only be discussed briefly.

A jump, J, is defined as a price that is higher than the mean plus or minus three times the standard deviation of the price series. Jumps were extracted using a numerical algorithm. The mean jump size and standard deviation are shown in Table 2. The Poisson parameter, λ, is defined as the mean time between a jump (defined above) in the price series and was estimated using the filtered jump prices. The jumps were isolated from the original price series, but the time series was maintained in order to determine the time between jumps. The distribution of the jumps follows the Poisson distribution (higher frequency at lower values). The Poisson parameter, λ, was calculated from the distribution of the times between jumps. The majority of time between jumps was below 200 h, or 8 days, with only six occurrences greater than 200 h. The Poisson parameter, shown in Table 2, indicates that there was, on average, one jump in price every 24 h.

The mean reversion speed, κ_t, mean reversion level, θ_t, and volatility, σ_t, parameters are typically estimated using linear regression [18,36]. In this case, the price series was filtered of jumps and, to maintain the time series, the filtered values were replaced with prices that were interpolated between the non-jump values. S_{t+1} were regressed against S_t because of the discretization of the mean-reverting model in Eq. (5) [36]:

$$S_{t+1} = (1-\kappa_t \Delta t)S_t + \kappa_t \theta_t \Delta t + \varepsilon \quad (5)$$

where ε represents the error of the regression. The slope was then used to find the mean-reversion speed which was estimated for each hour of the day for a given month, with $\Delta t = 1$.

Table 1
Electricity price summary statistics for HOEP between May 1, 2002 and June 30, 2009. The mean, maximum and minimum have units of $/MW-h (CAD).

Mean	51.17
Standard deviation	33.86
Maximum	1891.14
Minimum	−52.08
Skewness	7.21
Kurtosis	209.17

Table 2
Jump parameters—mean, standard deviation, and poisson parameter of the HOEP between May 1, 2002 and June 30, 2009.

μ_J ($/MW-h)	σ_j	λ (h)
154.85	81.13	24.26

The intercept was used to find the mean reversion level, θ_t, and was also calculated each hour of the day for a given month. The standard deviation of the residuals of this regression was used to find the volatility, σ_t, on the same time basis, as well. In order to maintain the different levels of seasonality present in the spot price dataset, the mean reverting levels and volatility were calculated separately for each hour in a day and for each month in a year.

2.3. Weather conditions

2.3.1. Markov-chain weather occurrence model

The stochastic weather model described here will be called the *cloud occurrence model* (COM). The COM is a modification of the ROM [30–32], which was described previously. This analysis simplified weather observations in that all precipitation events were considered "cloudy" and all conditions described as "mostly cloudy", "partly cloudy", and "clear" were considered "clear". This approach was validated in Powell et al. [17].

When it is cloudy, the irradiance that is available to the PV array is reduced, as is true for most PV technologies. This reduction was quantified in Powell et al. [17] by a CMF, which is a factor that determines the reduction in clear-sky solar irradiance during cloudy periods. The COM determines whether the next hour is cloudy or clear, depending on the current and previous hour(s) and multiplies the predicted clear-sky irradiance from the SMARTS2 model [37] by the CMF to determine the actual irradiance for that hour (as seen in [17]).

The COM also accounts for correlations to the electricity price model. Typically, it is assumed that the electricity price is driven partly by the weather, for example, extreme temperatures often leading to higher electricity prices [33,38–40]. For ease of implementation in the COM, the electricity price is assumed to be the independent variable so that the synthetic weather dataset is driven by changes in the electricity price, which is not intuitive. However, we believe this approach is equivalent to generating the weather series first and then generating a spot price based on the correlation (which is the intuitive physical interpretation; weather can affect electricity prices).

2.3.2. Parameter estimation

The following section will explain the procedure for determining the synthetic weather dataset using the electricity price correlation. The data used in parameter estimation for the synthetic weather series will be discussed. As well, the methods used to obtain the various parameters needed for the TEEOS algorithm will be introduced. These parameters include the order of the Markov-chain for the weather series, conditional frequency of various weather state sequences, the deviation of the actual electricity price from the mean electricity price and the associated distribution variables (mean, variance, etc.) to correlate the electricity price and weather model parameters.

The underlying weather data for the stochastic weather model was obtained from Environment Canada [41]. The cloudy and clear designations were from observational data at the Downsview weather station in Toronto, Ontario, Canada. 62 112 hourly observations were used, from May 1, 2002 at 12:00 am to May 30, 2009 at 11:00 pm. As mentioned previously, the data was adjusted to only include two weather observations, cloudy and clear.

The COM uses Markov-chain logic to determine the future state of the weather based on the current and previous states. The number of previous hours taken into account represents the order of the Markov-chain model. A graphing technique was used to

determine the order of the Markov chain, similar to Pattison [42] and Nkemdirim [43].

To implement the graphing technique for determining the Markov order, the probability that a current cloudy hour, $t+1$, was preceded by $t=1, 2, 3, \ldots, n$ clear hours, was found. In order to do this, a cloudy hour, $t+1$, preceded by 1 clear hour was separated from a cloudy hour, $t+1$, preceded by 2 clear hours; or more generally, any cloudy hour, $t+1$, preceded by n clear hours was divided into n different groups [42,43]. The conditional probability for each of these classifications was determined as follows:

$$\Pr\{h_{t+1}=\text{cloudy}|h_{t_n}=\text{clear}\}=\frac{f_i'}{F} \tag{6}$$

where f_i is the frequency with which a cloudy hour $t+1$ is preceded by clear hours $t_n=1, 2, \ldots, n$ and F is the sum of the frequencies.

As with the electricity prices, the weather states were binned by each month of the year, and the probabilities were calculated on a per month basis in an effort to account for seasonality. There was stabilization of the conditional probabilities around the sixth hour, which signified that the state of hour $t+1$ was dependent only on the sequence of states from hour t through to hour $t-5$. There was also a noticeable seasonality in the conditional probability curves, which justifies the monthly division of the data.

According to the graphing method, the COM for Toronto, Canada, was a sixth-order Markov process. However, it is shown in Table 3 that there was no significant difference in the annual savings calculation between using a sixth-order model and using a second-, third-, fourth-, or fifth-order Markov model with respect to the annual savings calculation. As a result, a third-order model was chosen for this paper because of a lower test value than the other orders and because it required less data and time to implement.

The approach to determine conditional probabilities used in this paper was different than that described by Pattison [42] and Nkemdirim [43]; here, it was adapted in order to model the occurrence of cloudy or clear skies, not the amount of rainfall, and also to account for the dependence with electricity prices, as discussed earlier. The procedure for this parameter estimation follows.

For a third-order Markov chain, the frequency of a given three hour sequence of weather (from t-2 to t) preceding either a cloudy or clear hour, $t+1$, must be found in order to determine the state at hour $t+1$ for a synthetic weather dataset. Therefore, to generate the synthetic weather series for this paper, four one-hour sequences of real data were binned according to 16 (2^4) possible combinations of states. For example, one sequence is cloudy, cloudy, cloudy, cloudy or, more simply, 0000 (0 is cloudy, 1 is clear).

For each electricity price in the historical data, a value ΔS_θ, which is the deviation of the electricity price from the mean of electricity prices, was calculated according to the following equation:

$$\Delta S_\theta = S_t - \theta_m \tag{7}$$

where S_t represents the historical electricity price for a given hour, t, θ_m represents the mean reversion level of the electricity price at the same time. The state of the historical weather for hour t and the three preceding hours was associated to the ΔS_θ at t. This separated each ΔS_θ into one of 16 possible sequences. For each vector of ΔS_θ associated to a specific weather sequence, a specific normal distribution was fit as follows. As an example, the histogram for ΔS_θ for the weather sequence 0100 (one cloudy day, one clear day and one cloudy day followed by a cloudy day) in January is shown in Fig. 1.

The histogram showed a distribution close to that of Gaussian. This "almost"-Gaussian distribution occurred throughout the dataset and as a result, the distributions of each vector of ΔS_θ were fit to some combination of two normal distributions in order to provide greater accuracy when determining the probability density. The function used for fitting is the following:

$$\Phi = w_1\Phi(\mu_1,\sigma_1)+w_2\Phi(\mu_2,\sigma_2) \tag{8}$$

where w_1 and w_2 are the weightings of the first and second normal distribution, respectively, with the restraint:

$$w_1+w_2=1 \tag{9}$$

where Φ represents the cumulative distribution function (CDF), μ_1 and μ_2 represent the means of the first and second normal distributions, respectively, and σ_1 and σ_2 represent the standard deviations of the first and second normal distributions, respectively. The fit was performed in Matlab using an algorithm that minimizes the total error of the fitted function through numerous iterations. Fig. 2 shows the sorted ΔS_θ vector for the sequence 0100 in January normalized by the length of the vector in blue and the fitted function P in red.

This fitting was done for each of the 16 possible weather sequences for each month in the historical dataset, giving five parameters, w_1, w_2, μ_1, μ_2, σ_1 and σ_2 for each, and 960 in total.

2.3.3. Synthetic weather series generation

The parameters in the previous section were determined from the underlying historical data. These parameters were then used to generate a synthetic weather series to use in the TEEOS algorithm to provide greater flexibility in performing sensitivity analyses over previous methods [17]. The following procedure was used:

1. Generate the synthetic electricity price series using the methods discussed in Section 2.2.2.
2. Calculate the ΔS_θ parameter for each datapoint in the synthetic price series, using the synthetic prices for S_t and the historical θ_m and Eq. (7).

Table 3
Student's t-test for difference of mean of annual savings with respect to Markov order for weather model.

Markov order	Mean annual savings ($)	T-stat (6th order control)	Critical value	Significant difference?
2	85.79	−0.3228	1.646	N
3	85.81	0.0356	1.646	N
4	85.80	−0.2001	1.646	N
5	85.75	−1.372	1.646	N
6	85.81	–	–	–

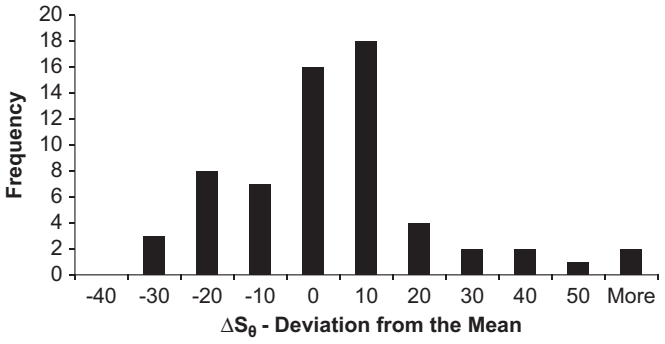

Fig. 1. Histogram of ΔS parameter for weather sequence 0100 in January.

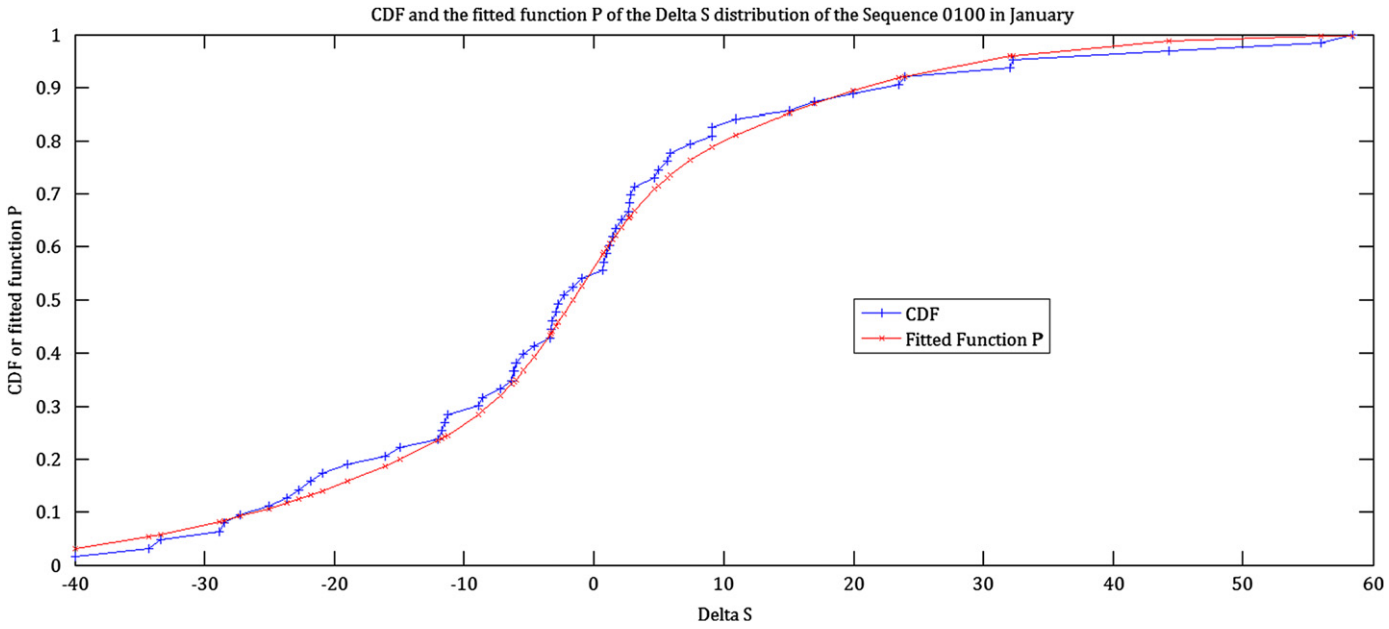

Fig. 2. CDF and the function Φ from Eq. (6) of the ΔS distribution of the Sequence 0100 in January. The *R*-squared value for the fit is 0.9957.

3. Begin by assuming that the first three hours in the synthetic weather series are 000, that is, they are all cloudy (any sequence will work, but 000 is the simplest).
4. Calculate the probability density, p_0, for the sequence 0000, given the ΔS_θ for that next hour using the five distribution fit parameters for the sequence 0000 in the required month as follows:

$$p_0 = w_1\phi(\Delta S_\theta,\mu_1,\sigma_1)+(1-w_1)\phi(\Delta S_\theta,\mu_2,\sigma_2) \quad (10)$$

where ϕ represents the probability density function (PDF) and $\phi(\Delta S_\theta,\ \mu,\ \sigma)$ is the PDF of a distribution with mean, μ, and standard deviation, σ, evaluated at the value ΔS_θ.
5. Calculate the probability density, p_1, that the state of the next hour will be 1, given the same ΔS_θ, but using the five distribution-fit parameters for the sequence 0001 in the required month, according to Eq. (10).
6. Scale the two probabilities, p_0 and p_1, by multiplying them by their respective proportional frequencies calculated previously as such:

$$p_0^* = p_0(f_0/f_0+f_1) \quad (11)$$

$$p_1^* = p_1(f_1/f_0+f_1) \quad (12)$$

7. Calculate the probability, P_0:

$$P_0 = p_0^*/p_0^*+p_1^* \quad (13)$$

8. Generate a uniformly random number. If it is less than P_0, then the state of hour $t+1$ is 0 or cloudy, if it is greater, the state of hour $t+1$ is 1 or clear.
9. Move to the next hour and repeat starting at Step 4 for the duration of the required time period.

2.4. Verification of models

2.4.1. Verification of electricity price model

The electricity price simulation was run 15,000 times for one simulated year and, for verification, the parameters of the synthetic price sets were determined using the same method of obtaining the parameters from the historical price dataset, as described above. There was a slight difference in the parameters for the synthetic electricity price than for the historical dataset. Each monthly synthetic mean reversion speed was slightly larger than its corresponding historical mean-reversion speed. This means that the synthetic prices take a shorter time to return to their respective means than the historical prices. This effect was most powerful after a jump. The difference between the synthetic and historical parameters did not significantly affect the price dynamics, however, possibly because the time between jumps in the synthetic price series was higher as well. The mean jump in the synthetic electricity price was slightly lower than the historical dataset, with a higher standard deviation, implying a higher volatility than the historical dataset. The time between jumps in the synthetic data set was considerably longer than the historical dataset. This can be explained by the large number of jumps that occurred in succession in the historical dataset; if three jumps (as defined by the procedure above) occur in succession, the time between jumps is one hour. If a lot of the jumps in the dataset are in succession, it reduces the Poisson parameter. When using this parameter to generate a synthetic dataset, the randomly generated numbers will not behave exactly the same as the historical process because the jump process is not *exactly* a Poisson process, just an estimation of the distribution of the times between jumps.

2.4.2. Verification of stochastic weather model

Verification of rainfall occurrence models typically involved comparing the length of dry and wet spells and comparing the distribution of rainfall amounts during wet spells [31,44]. With the COM, the verification involved comparing the length of cloudy and clear spells and the overall ratio of cloudy and clear hours between the historical weather series and the synthetic weather series.

Table 4 shows the probability of cloudy spell lengths and clear spell lengths for both the synthetic and historical weather series. Table 5 shows the regression analysis between the historical and synthetic weather series for cloudy and clear spell lengths. As shown in Table 5, there is a stronger correlation between the historical and synthetic weather series for clear spell lengths than cloudy spell lengths. In the historical dataset, there are considerably longer spells of cloudy hours than in the synthetic weather

series; over 17% of cloudy spells in the historical weather series are over 10 h, while only 3% are greater than 10 h in the synthetic dataset. This likely occurs because of the assumption of the dependence of the synthetic weather series on the electricity price series. This assumption may affect the accuracy of the probability of a longer cloudy spell length in the synthetic weather series because a lower frequency of cloudy hours would affect the accuracy of fitting the cloudy state/electricity price distributions. The clear spell lengths seem to agree quite well, however, with a high correlation coefficient and R^2 between the historical and synthetic weather series.

In the historical weather series, there were 21,496 (35%) cloudy hours and 40,616 (65%) clear hours. In the synthetic weather series, with 1000 iterations, there are on average 2981 (34%) cloudy hours and 5779 (66%) clear hours, per year. This shows that the stochastic model chosen did follow the general trend of the historical weather series.

2.5. The sample solar cells

The TEEOS model used in this paper differs from that in Powell et al. [17] due to the addition of correlated stochastic models to determine electricity price and weather patterns, as opposed to using only one year of historical data. As well, an enhancement of the model has been made so that the EQE is used in order to perform a more robust sensitivity analysis. This modified TEEOS model was used to analyze the power production and economic feasibility of three solar cells: one Silicon-based and two OPVs (one dye-sensitized and one polymer). A summary of the technological characteristics of the three solar cells is shown in Table 6. It should be noted that the areas of the sample cells that were chosen were much smaller than the assumed size here. It is also recognized that when scaling the cells up, for example, from 0.219 cm^2 to 10 m^2 in the case of the DSSC [58], that the same efficiencies would simply not be possible. The analysis in this paper assumes that this scale-up is possible and necessary to achieve economic feasibility in the field. It is also recognized that the cost of these smaller experimental cells may not fall under the ranges listed in Table 6, but comparable costs are simply not available.

The main output of the model is the annual savings accrued based on the avoided cost of electricity by using PVs for domestic electricity use. Using the annual savings, the NPV was calculated and is presented in this section. A range of cell and ancillary costs, known as fixed costs, are given in Table 6; in this analysis, however, a uniformly distributed random value for the fixed costs between the given range was chosen when determining the NPV. The interest rate used for NPV was 2% and an annual electricity price escalation factor, γ, of 2% was used. In addition, the cell degradation was modeled as a straight line from peak efficiency to 80% of the peak efficiency at the end of its lifetime. The lifetime of the cells varies as shown in Table 6; the lifetime of the Si-based cell is 25 years, whereas the OPVs have a lifetime of only 5 years: this reflects the instability of the organic PVs relative to the Si-based PVs. The EQEs for each cell are not shown here for brevity but are available from the references cited for each cell in Table 6.

Table 4
Cloudy and clear spell probabilities of various lengths for historical and synthetic weather series. Synthetic weather series completed with 1000 iterations.

Run length (H)	Cloudy spell length probabilities		Clear spell length probabilities	
	Historical	Synthetic	Historical	Synthetic
1	0.3348	0.3187	0.3500	0.3730
2	0.1528	0.2547	0.1667	0.2594
3	0.0989	0.2427	0.1000	0.0588
4	0.0742	0.0693	0.0833	0.0374
5	0.0427	0.0307	0.0500	0.0294
6	0.0382	0.0173	0.0333	0.0240
7	0.0270	0.0120	0.0333	0.0201
8	0.0247	0.0080	0.0333	0.0174
9	0.0202	0.0067	0.0167	0.0147
10	0.0157	0.0053	0.0167	0.0120
Over 10	0.1708	0.0347	0.1167	0.1658

Table 5
Regression analysis between wet spells and probabilities of various sequence length for historical and synthetic weather series. Synthetic weather series completed with 1000 iterations.

Weather condition	Correlation coefficient	R^2	Standard error of estimate
Cloudy	0.7995	0.6391	0.0754
Clear	0.9551	0.9122	0.0380

3. Results

The following results are shown in this section: (1) the annual power production and net present value (NPV) for the three solar cells over a 25-year time horizon; (2) the annual power production and NPV of the two OPVs over a 5-year horizon using synthetic and historical price and weather data; and (3) a sensitivity analysis on the inputs to the modified TEEOS model using only the third polymer-based solar cell, including an examination in varying the EQE in the incident spectrum.

3.1. Annual power and NPV

First, the three cells were examined over a 25-year horizon. This means that because the OPVs (cells 2 and 3) only have a lifetime of 5 years, they had to be purchased again areat years 5,

Table 6
Technological characteristics of three sample solar cells.

Characteristic	Silicon	DSSC	OSC
Incident spectrum (approx.)[a]	280–1200 nm [56,57,59]	300–950 nm [58,59]	280–800 nm [59]
Efficiency	24.4% [56,57,59]	11.2% [58,59]	10.0% [59]
V_{OC}	0.696 [57]	0.737 V [58]	0.899 V [59]
FF	83.6% [57]	72.2% [58]	66.1% [59]
I_{SC}	42.0 mA/cm^2 [57]	21.0 mA/cm^2 [58]	16.75 mA/cm^2 [59]
Cell lifetime	25 years	5 years	5 years
Assumed cell area	10 m^2	10 m^2	10 m^2
Cost of cell	\$250/m^2–300/m^2 [49]	\$37/m^2–158/m^2 [6]	\$49/m^2–\$139/m^2 [6]
Balance of System (BOS) costs	\$40/m^2–75/m^2 [6,48]	\$40/m^2–75/m^2 [6,48]	\$40/m^2–75/m^2 [6,48]

[a] The EQE of each cell can be found in their respective references for the incident spectrum.

10, 15 and 20. The mean power production (kWh/year) and the NPV, as well as 95% confidence intervals, are shown for each of the three cells in Fig. 3. 1000 iterations of the synthetic data series as well as the CMF and cell costs were used for all results in this paper.

The Si-based cell has much higher efficiency than the other cells and thus has a much higher annual power production than the other cells. The OPVs have similar power production because they have similar overall efficiencies. In Fig. 3b, the NPV of the Si-based cell is positive and high because of the high power production. The OPVs have a negative NPV because of the need to purchase 5 systems over the time horizon and the low power production. In terms of power production or NPV, the OPVs do not perform very well compared to the Si-based solar cell.

Next, the two OPVs were examined over a 5-year horizon and both synthetic and actual electricity prices and weather were used. The mean power production and the NPV are shown for each of the cells in Figs. 4a and b, respectively. For both OPVs, the synthetic data series under predicted the power production by approximately 7%. However, the NPV of each cell using the synthetic data series is slightly higher than that using the historical data. This difference is due to the time period chosen for the historical electricity price and weather series. For the actual data, the years 2006–2010 were used, whereas the synthetic data series was trained on electricity prices and weather from 2002–2009. The average price of electricity was approximately 8% higher over the eight-year period on which the synthetic data series was trained, so the NPV should be slightly higher for the synthetic dataset. As well, there were fewer daytime cloudy hours annually for the time period 2006–2010 then the training period, so the power production should be higher for the historical dataset. This contradiction may occur regardless of the 5 years of actual data: the shortened time period would not necessarily reflect the performance over the longer time period. The long training period was not reduced to match the five-year horizon in order to keep the analysis standard for all of the results.

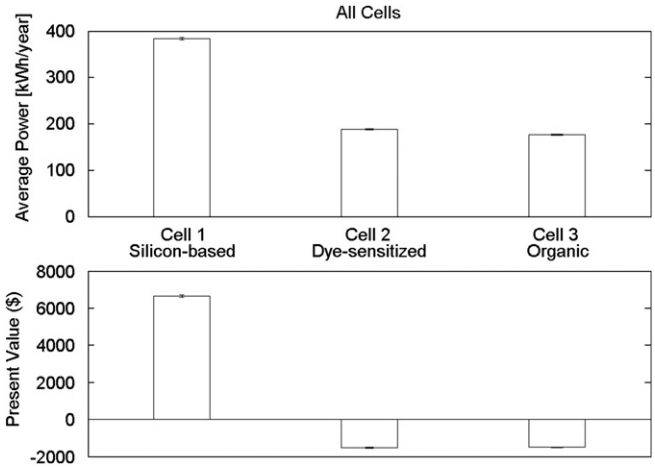

Fig. 3. (A) Mean power production [kWh/yr] for each of the three cells (left to right): Si-based, DSSC, OSC with 95% confidence intervals. (B) Mean NPV {$} for each of the three cells with 95% confidence intervals based on 1000 iterations. 1000 iterations and a 25-year time horizon were used.

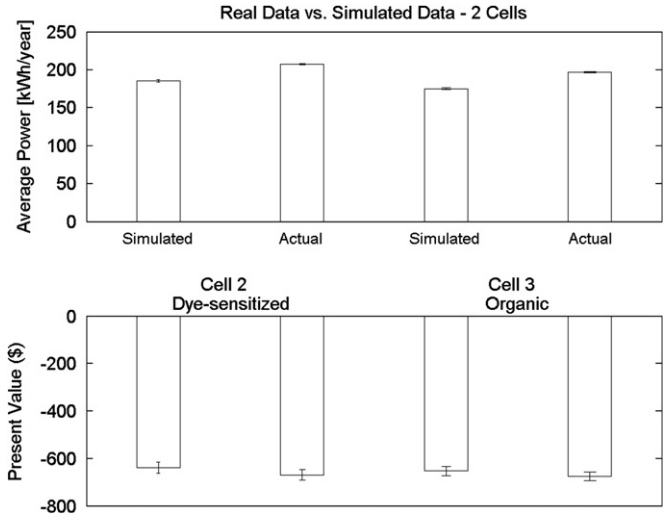

Fig. 4. (A) Mean power production [kWh/yr] for the DSSC (first two bars) and OSC (last two bars) with 95% confidence intervals. For each cell, the first bar represents the synthetic weather and electricity price series and the second bar represents the historical or actual weather and electricity price series. (B) Mean NPV ($) for the DSSC and OSC with the same conditions as Fig. 4A. 1000 iterations and a 5-year time horizon were used.

3.2. Sensitivity analysis

The ability to perform a robust sensitivity analysis using the modified TEEOS model is the main advantage over its simpler predecessor in Powell et al. [17]. This section examines the difference to power production and NPV using three sensitivities: (1) changes in the price escalation factor; (2) removing the correlation between the weather series and electricity prices; and (3) removing the jumps in the electricity prices. Only the third cell, the OSC, was used for this analysis and a five-year time horizon was used. The power production and NPV are shown for all sensitivities in Fig. 5a and b, respectively. The first two bars (from left to right) represent the power production and NPV of the OSC using the historical weather and electricity prices and the OSC using the synthetic data series, respectively.

3.2.1. Electricity price escalation

In light of the possibility of more expensive electricity in the future, it is important to model inherent increases in the electricity price. An escalation factor, γ, was used in Eq. (1) to address

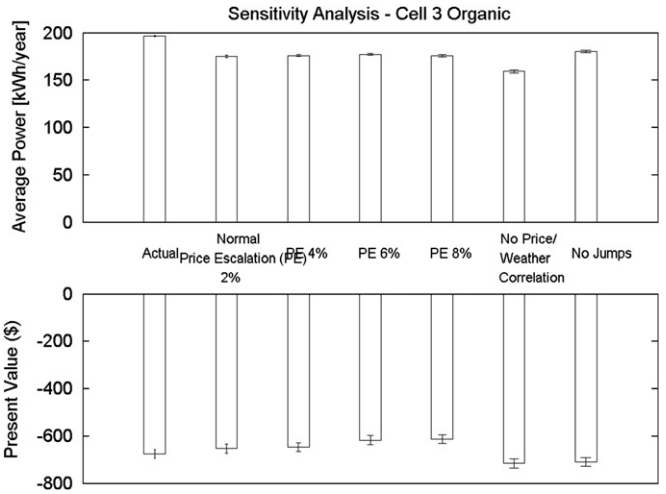

Fig. 5. (A) Mean power production [kWh/yr] for the OSC using a number of sensitivities with 95% confidence intervals. From left to right, the bars show (1) the historical weather and electricity price series; (2) the synthetic weather and electricity price series; (3, 4, 5) the price escalation factor of 4, 6, and 8% respectively; (6) no correlation between the weather and electricity price; and (7) no jumps in the electricity price model. (B) Mean NPV ($) for the OSC with the same conditions as Fig. 5A. 1000 iterations and a 5-year time horizon were used.

changes in electricity prices due to structural changes, such as new generation capacity and transmission lines. Throughout the results shown in this paper, the annual escalation of prices is set at 2%. However, recent reports show that electricity prices in Ontario, Canada will increase 46% over the next five years with an annual rate of approximately 8% [45]. This analysis looked at annual increases to the mean reverting level, θ_t, of 4, 6, and 8%. It was assumed here that wholesale electricity prices in Ontario would not decrease in the future so a negative escalation factor was not tested.

In Fig. 5, bars 3, 4, and 5, (from left to right) show the power production and NPV of the OSC using 4, 6, and 8% price escalation factors, respectively. In Fig. 5a, the power production does not change significantly as the mean price increases. This is because the same escalation factor is used in the synthetic weather production algorithm. In Fig. 5b, however, the mean NPV increased slightly as the mean price increased.

3.2.2. Correlation of weather to electricity prices

A further validation of the stochastic weather model used in this paper is to determine the difference in the financial indicators when removing the correlation between the weather and the electricity prices. Previously in this paper, the method for determining the correlated weather series was outlined. This involved using a distribution of electricity prices correlated to a specific weather series to determine the weather condition at a specific hour. For the non-correlated weather series, electricity prices are not correlated with a specific hourly weather condition. The process for generating such a weather series depends solely on past weather condition data. The procedure for this was outlined by Pattison [42] and Nkemdirim [43] and will not be detailed here, but is straightforward to implement with our model.

Fig. 5 shows the mean annual power production (Fig. 5a) and the NPV (Fig. 5b) using the non-correlated weather series. The non-correlated power production was considerably less than the historical power production (Bar 1) and the correlated power production (Bar 2). As a result, the non-correlated NPV was lower than normal. Without an actual demonstration to compare, it is difficult to make conclusions, but this suggests that the correlated weather series reflects the historical data better than the non-correlated weather series results and makes the model results more precise.

3.2.3. Modeling without jumps

To investigate sensitivity in the electricity price model, the modified TEEOS model was run using a stochastic electricity price model that did not model jumps. The equation used for this sensitivity analysis is shown here:

$$dS_t = \kappa_t(\theta_t - S_t)dt + \sigma_t dZ_t \tag{14}$$

The same parameters used in Eq. (4) are used here, except the jump term is removed.

In Fig. 5, bar 7 shows the mean annual power production and the NPV of the OSC. It can be deduced that the average and standard deviation of the electricity prices *without* jumps will be lower than the average and standard deviation of the electricity prices *with* jumps. The extremes in prices caused by the jumps did not exist in this case, which lead to a lower NPV. The mean-reverting jump diffusion model is the appropriate model to simulate the electricity prices in this modified TEEOS model.

3.3. Enhancement and expansion of the incident spectrum

An important consequence of modifying the TEEOS model is the ability to perform a sensitivity analysis on the incident spectrum. In the modified TEEOS model, the EQE is used in order to get total power efficiency at each wavelength. With a number of assumptions, we can increase the EQE in the existing incident spectrum of the OSC (what we call enhancing the incident spectrum) or reduce the band gap of the existing incident spectrum of the OSC (what we call expanding the incident spectrum) in order to determine the effect on the financial indicators.

3.3.1. Enhancement of the incident spectrum

The enhancement of the incident spectrum using the modified TEEOS model is meant to simulate the use of a material or dye or technique, such as annealing that would improve the EQE of the solar cell within the existing incident spectrum. In this paper, we increased the EQE of the OSC by 5, 10, 15, 20 and 30% and examined the effect on power production and NPV. The maximum possible EQE at any wavelength was 100%. The open circuit voltage and the fill factor were kept constant, as was used in Klampaftis et al. [49]. Without any experimental validation, this assumption is made to simplify the analysis.

In Fig. 6, the bars from left to right show the power production (Fig. 6a) and the NPV (Fig. 6b) of the OSC using 0, 5, 10, 15, 20 and 30% enhancement of the EQE. When the EQE is increased, the short-circuit current is increased. With the assumption that the open circuit voltage and the fill factor are constant, any increase in the EQE should lead to an increase in the overall efficiency. This is reflected in the increased power production as the enhancement increases. The power production increases about 20% with the enhancement of the incident spectrum by 30%. The NPV increases by about 16% with the enhancement of the incident spectrum by 30%.

3.3.2. Expansion of the incident spectrum

The expansion of the incident spectrum using the modified TEEOS model is meant to simulate the use of a new material or dye with a lower band gap that would increase the range of the EQE of the OSC. In this paper, we reduced the band gap of the OSC, which was estimated as the energy of the wavelength at which the EQE drops below 50% of its peak value [59]. Each time the band gap was reduced, the slope of the curve in the long wavelengths that connected the peak EQE to the minimum EQE (usually zero) was changed to fit the new band gap. The band gap was reduced by 5, 10, 15, 20 and 30% and the effect on power production and the NPV was examined. Again, the open circuit voltage and the fill factor were kept constant.

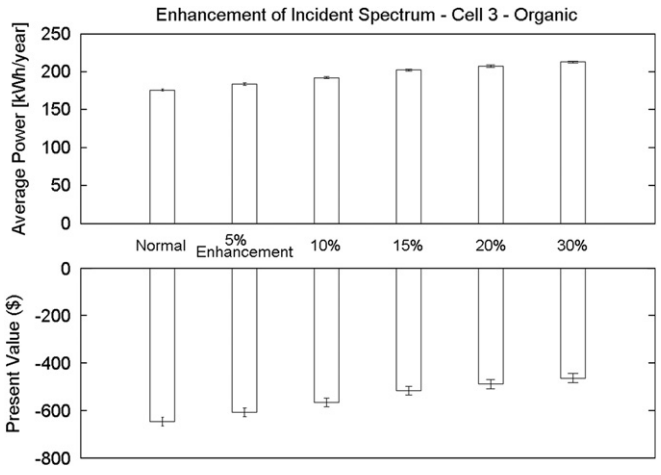

Fig. 6. (A) Mean power production [kWh/yr] for the OSC with enhancement of the incident spectrum with 95% confidence intervals. From left to right, the bars represent 0, 5, 10, 15, 20, and 30% enhancement of the incident spectrum. (B) Mean NPV ($) for the OSC with the same conditions as Fig. 6A. 1000 iterations and a 5-year time horizon were used.

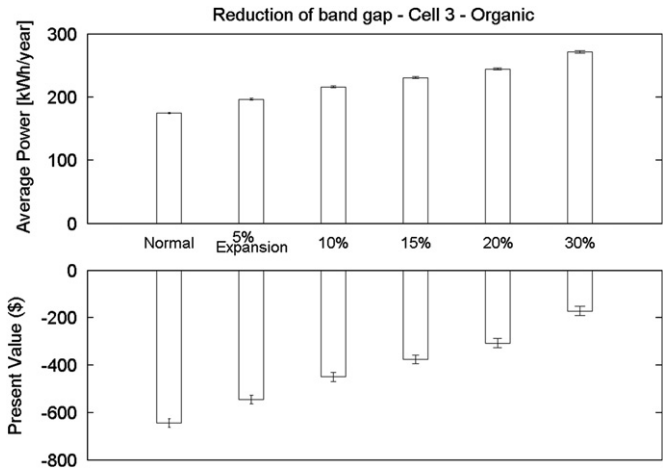

Fig. 7. (A) Mean power production [kWh/yr] for the OSC with expansion of the incident spectrum with 95% confidence intervals. From left to right, the bars represent 0, 5, 10, 15, 20, and 30% expansion of the incident spectrum. (B) Mean NPV ($) for the OSC with the same conditions as Fig. 7A. 1000 iterations and a 5-year time horizon were used.

In Fig. 7, the bars from left to right show the power production (Fig. 7a) and the NPV (Fig. 7b) of the OSC using 0, 5, 10, 15, 20 and 30% expansion of the EQE. When the EQE was expanded, the overall efficiency in this case increased. This is not always the case, as shown in [55], but it was a safe assumption here. This is reflected in the increased power production as the expansion increases, which is seen in Fig. 7a; it is much more pronounced than with the simple enhancement seen in the previous section. The power production increases about 60% with the expansion of the incident spectrum by 30%. The NPV increases by about 70% with the 30% expansion. The expansion of the EQE is clearly the best way to improve economic feasibility of the solar cells. This can be done in many ways, especially using new low band gap polymers, but this is not the focus of this paper. The reader is directed to a sampling of the literature [49–55].

4. Technical objectives

One of the important outcomes of using the TEEOS model is the ability to determine technical objectives for PV using the financial indicators. The technical objectives discussed here are technical benchmarks or targets that can be used as a goal for researchers to produce OSCs that are financially feasible based on the current analysis for Toronto, Canada; however, these recommendations are certainly applicable all over the world. Analyses will be made on the major inputs of the TEEOS model: fixed costs of an organic solar array, the EQE and incident spectrum of the cells, electricity prices, and the lifetime of the cells.

4.1. Fixed costs

The fixed costs of the organic solar array are made up of the solar cell costs and the balance of system (BOS) costs. This analysis will use the results previously presented to develop recommendations regarding target fixed costs. To achieve a NPV = 0, for the third cell, the fixed costs of the array would need to be approximately $\$87/m^2$, which is certainly at the low range of the costs of the cells used in this paper (see Table 6). Assuming that approximately 50% of the fixed costs are the solar cell costs (the minimum of the range used here), the costs of the OSC, themselves, would need to be $< \$45/m^2$ to have a positive NPV. This is certainly a reasonable goal.

The detailed costing of organic solar cells is still very preliminary, as most cell types have not yet been developed for commercialization, but costs are becoming more available [4–6,8]. The costs of the cells used in this paper were for small production that did not take advantage of econonies of scale. With better technology to produce these solar cells on a large scale, it is conceivable that cell costs could be reduced below $\$40/m^2$. There is high potential for OSCs to be a very low-cost emerging energy technology; low-cost printing press production techniques, non-commodity organic materials, and adaptability and flexibility, make OSCs an attractive technology for energy harvesting. Krebs et al. [5] notes that the price of organic solar cells may be under $\$2/m^2$ within the next ten years. Indeed, it is safe to assume that if the OSC were tested in a locale closer to the equator and with more sunny days than Toronto, the price point for OSC to achieve a positive NPV would be even lower.

4.2. Incident spectrum

An OSC with a higher total power efficiency should by definition provide a higher power production and NPV. This was seen in the sensitivity analysis where the incident spectrum was both enhanced and expanded which lead to a higher EQE and thus a higher total power efficiency. Although there were a number of assumptions made here regarding the voltage and fill factor as well as the costs of the enhanced cells, this certainly provides a lesson on the direction the OSC field needs to go in order to achieve economic feasibility. Even with a 30% enhancement or a 30% expansion, the NPV was still negative. However, with more strategic pairing of polymers and dyes that enhance or expand the incident spectrum, or with cheaper materials, this problem can be overcome.

4.3. Electricity prices

An interesting result of the modified TEEOS model is the ability to see patterns in the way the electricity price and the weather interact. In the modified TEEOS model, the electricity price changes depending on the weather. When the weather is cloudy, the cost of electricity is approximately $2/MWh cheaper than when the weather is clear for the synthetic data set trained using data from 2002–2009. This is important because when the solar panel is generating the most power (i.e. when the weather is clear and sunny), the price of electricity that it is offsetting is *higher*. This is a significant result, but certainly requires more examination especially with respect to different locales.

4.4. Cell lifetime

In the results presented here, the lifetime of the OSCs was assumed to be 5 years. This is slightly longer than the best achieved laboratory lifetime for an OSC, estimated at 20, 000 h [46]. Lifetimes of 10,000 h have been reached by very small cells in standard sunlight conditions [47]. If OSCs can achieve longer stability, the NPV of the cells will undoubtedly improve; this is one of the barriers to commercialization. Considerable effort should be made to increase the stability of the organic solar cell [1,2,17]. A longer cell lifetime is most desirable to homeowners; if one desires a 25-year project lifetime, currently, the purchase of five organic solar cell systems would be required, reducing the NPV considerably (as was shown in Fig. 3). As more research is done on the stability of polymers and plastics in different outdoor conditions, a variety of cells can be developed that suit different climates and locations, but in order to compete with traditional solar technologies, a much higher lifetime is necessary.

5. Conclusions

A modified TEEOS model with two stochastic models for electricity prices and weather and with the introduction of EQE as an input was introduced in this paper in order to obtain a more robust sensitivity analysis of results that that shown in Powell et al. [17]. A mean-reverting jump diffusion model was used to model the electricity price of Toronto, Canada, and while some parameters of the synthetic electricity price series deviated from that of the historical price series, the final results showed that the electricity price model was adequate. A third-order Markov-chain cloud occurrence model was used for the generating the synthetic weather series and the series matched well with the actual weather series in that time period. Through the variation of the parameters in the stochastic models, a wide sensitivity analysis was obtained and technical objectives for the OSCs were discussed.

- Si-based cell outperformed the DSSC and OSC in power production and NPV, as expected.
- Using the synthetic weather and electricity series and actual data produced similar results, although slight differences were caused by different time periods.
- An increase in the electricity price over time did not cause a significant change in the power production nor the NPV.
- Removing the correlation between the weather and electricity prices caused a reduction in power and NPV and showed that the correlation was necessary.
- Removing the jumps in the electricity price model also reduced the NPV and showed that the mean-reverting jump diffusion model was necessary.
- Higher electricity prices are seen in clear weather in Toronto for the period study, which only serves to help the economics of the OSC.
- Reducing the band gap (i.e. expanding the EQE) of the incident spectrum of solar materials would produce higher power production and NPV than increasing the existing EQE, but both approaches should be explored to increase economic feasibility.
- The break-even point for OSCs in Toronto, ON is about $\$40/m^2$ for the cells alone. This is definitely achievable and is on the low range of estimates currently available.

More work must be done to improve the lifetime of OSCs compared to Si-based PVs.

References

[1] C. Brabec, Organic photovoltaics: technology and market, Solar Energy Materials and Solar Cells 83 (2004) 273–292.

[2] B. Azzopardi, C.J.M. Emmott, A. Urbina, F.C. Krebs, J. Mutale, J. Nelson, Economic assessment of solar electricity production from organic-based photovoltaic modules in a domestic environment, Energy and Envrionmental Science 4 (2011) 3741–3753.

[3] S. Günes, H. Neugebauer, N.S. Sariciftci, Conjugated polymer-based organic solar cells, Chemical Review 107 (2007) 1324–1338.

[4] C.F. Krebs, M. Jørgensen, K. Norrman, O. Hagemann, J. Alstrup, T.D. Nielsen, J. Fyenbo, K. Larsen, J. Kristensen, A complete process for production of flexible large area polymer solar cells entirely using screen priting-First public demonstration, Solar Energy Materials and Solar Cells 93 (2009) 422–441.

[5] F.C. Krebs, T.D. Nielsen, J. Fyenbo, M. Wadstrøm, M.S. Pedersen, Manufacture, integration and demonstration of polymer solar cells in a lamp for the Lighting Africa initiative, Energy and Environmental Science 3 (2010) 512–525.

[6] J. Kalowekamo, E. Baker, Estimating the manufacturing cost of purely organic solar cells, Solar Energy 83 (8) (2009) 1224–1231.

[7] A.J. Medford, M.R. Lilliedal, M. Jørgensen, D. Aarø, H. Pakalski, J. Fyenbo, F.C. Krebs, Optics Express 18 (2010) S3.

[8] T. Nielsen, C. Cruickshank, S. Foged, T. Jesper, F.C. Krebs, Business, market, and intellectual property analysis of polymer solar cells, Solar Energy Materials and Solar Cells 94 (2010) 1553–1571.

[9] F.C. Krebs, S.A. Geyorgyan, B. Gholamkhass, S. Holdcroft, C. Schlenker, M.E. Thompson, B.C. Thompson, D. Olson, D.S. Ginley, S.E. Shaheen, H.N. Alshareef, J.W. Murphy, W.J Youngblood, N.C. Heston, J.R. Reynolds, S. Jia, D. Laird, S.M. Tuladhar, J.G.A. Dane, P. Atienzar, J. Nelson, J.M Kroon, M.M Wienkm, R.A.J Jannseen, K. Tvingstedt., F. Zhang, M. Andersson, O. Inganäs, M. Lira-Cantu, R. deBettignies, S. Fuillerez, T. Aernouts, D. Cheyns, L. Lutsen, B. Zimmermann, U. Wurfel, M. Niggemann, H.-F. Schleiermacher, P. Liska, M. Grätzel, P. Lianos, E.A. Katz, W. Lohwasser, B. Jannon, A round robin study of flexible large-area roll-to-roll processed polymer solar cell modules, Solar Energy Materials and Solar Cells 93 (2009) 1968–1977.

[10] R.W. Wies., R.A. Johnson, A.N. Agrawal, T.J. Chubb, Simulink model for economic analysis and evnrionmental impacts of a PV with diesel-battery system for remote villages, IEEE Transactions on Power Systems 20 (2) (2005) 692–700.

[11] A. Ucar, M. Incalli, A thermo-economical optimization of a domestic solar heating plant with seasonal storage, Applied Thermal Engineering 27 (2007) 450–456.

[12] J. Byrne, S. Letendre, C. Govindarajalu, Y.-D. Wang, Evaluating the economics of photovoltaics in a demand-side management role, Energy Policy 24 (2) (1996) 177–185.

[13] J.L Bernal-Agustín, R. Dufo-López, Economical and environmental analysis of grid connected photovoltaic systems in Spain, Renewable Energy 31 (2006) 1107–1128.

[14] S. Rehman, M.A. Bader, S.A. Al-Moallem, Cost of solar energy generated using PV panels, Renewable and Sustainable Energy Reviews 11 (2007) 1843–1857.

[15] T.T. Chow, A.L.S. Chan, K.F. Fong, Z. Lin, W. He, J. Li, Annual performance of building-integrated photovoltaic/water-heating system for warm climate application, Applied Energy 86 (2009) 689–696.

[16] RETScreen International. 〈http://www.retscreen.net〉, 2010 (accessed 01.09.10).

[17] C. Powell, T. Bender, Y. Lawryshyn, A model to determine financial indicators for organic solar cells, Solar Energy 83 (2009) 1977–1984.

[18] A. Cartea, M.G. Figueroa, Pricing in electricity markets: a mean reverting jump diffusion model with seasonality, Applied Mathematical Finance 12 (2005) 4.

[19] R. Huisman, C. Huurman, R. Mahieu, Hourly electricity prices in day-ahead markets, Energy Economics 29 (2007) 240–248.

[20] N.K. Nomikos, O. Soldatos, Using affine jump diffusion models for modeling and pricing electricity derivatives, Applied Mathematical Finance 15 (1) (2008) 41–71.

[21] R. Weron. Forecasting wholesale electricity prices: a review of time series models, in: Financial Markets: Principles of Modelling, Forecasting and Decision-Making, W. Milo, P. Wdowinski (Eds.), FindEcon Monograph Series, WUL, Lodz, 2008.

[22] A. Escribano, J. Peña, P. Villapana. Modeling electricity prices: international evidence, Working Paper 2:27. Universidad Carlos III de Madris, 2002.

[23] S. Borenstein, J. Bushnell, C. Knittel, C. Wolfram. Trading inefficiencies in California's electricity market, Working Paper PWP-086, University of California Energy Institute, Berkeley, 2002.

[24] Y. Li, P. Flynn, Deregulated power prices: comparison of volatility, Energy Policy 32 (2004) 1591–1601.

[25] Wolak. Market design and price behavior in restructured electricity markets: an international comparison, Working Paper, Department of Economics, Stanford University, 1997.

[26] B. Ramsay, A. Wang, A neural network based estimator for electricity spot pricing with particular reference to weekends and public holidays, Neurocomputing 23 (1) (1997) 47–57.

[27] C.P. Rodriguez, G.J. Anders, Energy price forecasting in the Ontario competitive power system market, IEEE Transactions on Power Systems 19 (1) (2004) 366–374.

[28] F. Nogales, J. Contreras, A. Conejo, R. Espinola, Forecasting next-day electricity prices by time series models, IEEE Transactions on Power Systems 17 (2) (2002) 342–348.

[29] S. Hikspoors, S. Jaimungal, Energy spot price models and spread options models, International Journal of Theoretical and Applied Finance 10 (7) (2007) 1111–1135.

[30] D.S. Wilks, R.L. Wilby, The weather generation game: a review of stochastic weather models, Progress in Physical Geography 23 (1999) 329–357.

[31] R.W. Katz, M.B. Parlange, Generalization of chain-dependent processes: application to hourly precipitation, Water Resources Research 31 (1995) 1331–1341.

[32] K.R. Gabriel, J. Neumann, A Markov chain model for daily rainfall occurrence at Tel Aviv, Quarterly Journal of the Royal Meteorological Society 88 (1962) 90–95.

[33] B.R. Rambharat, A.E. Brockwell, D.J. Seppi, A threshold autoregressive model for wholesale electricity prices, Applied Statistics 54 (2) (2005) 287–299.

[34] T.A. Johnsen, Demand, generation, and price in the Norwegian market for electric power, Energy Economics 23 (2001) 227–251.

[35] Independent Electricity System Operator. Hourly Ontario Electricity Price (HOEP), 〈http://www.ieso.ca/imoweb/marketData/marketData.asp〉, 2008 (accessed 08.08.08).

[36] L. Clewlow, C. Strickland, Energy Derivative: Pricing and Risk Management Lacima Publications (2000).
[37] C. Gueymard, Prediction and validation of cloudless shortwave solar spectra incident on horizontal, tiltied, or tracking surfaces, Solar Energy 82 (2008) 260–271.
[38] C.R. Knittel, M.R. Roberts, An empirical examination of restructured electricity prices, Energy Economics 27 (2005) 79–117.
[39] A. Boogert, D. Dupont, The nature of supply side effects on electricity prices: the impact of water temperature, Economics Letters 88 (2005) 121–125.
[40] R.F. Engle, C. Mustafa, J. Rice, Modelling peak electricity demand, Journal of Forecasting 11 (3) (1992) 241–251.
[41] Environment Canada. Canada's National Climate and Weather Data Archive. 〈http://climate.weatheroffice.ec.gc.ca/〉, 2008 (accessed 08.08).
[42] A. Pattison, Synthesis of hourly rainfall data, Water Resources Research 1 (4) (1965) 489–498.
[43] L. Nkemdirim, Simulating the rainfall process, The Canadian Geographer 18 (2) (1974) 139–147.
[44] R.W. Katz, On some criteria for estimating the order of a Markov chain, Technometrics 23 (1981) 243–249.
[45] Toronto Star Behind those rising hydro rates. 〈http://www.thestar.com/opinion/editorialopinion/article/1100094–behind-those-rising-hydro-rates〉, 2011 (accessed 23.12.11).
[46] E. Bundgaard, F.C. Krebs, Low band gap polymers for organic photovoltaics, Solar Energy Materials and Solar Cells 91 (2007) 954–985.
[47] M. Jørgensen, K. Norrman, F.C. Krebs, Stability/degradation of polymer solar cells, Solar Energy Materials and Solar Cells 92 (2008) 686–714.
[48] US Department of Energy, USDOE. Basic Research Needs for Solar Energy Utilization: Report of the Basic Energy Sciences Workshop on Solar Energy Utilization, 2005.
[49] E.,D. Klampaftis, K.R. Ross, B.S.Richards McIntosh, Enhancing the performance of solar cells via luminescent down-shifting of the incident spectrum: A review, Solar Energy Materials and Solar Cells 93 (2009) 1182–1194.
[50] A. Dhanabalan, J.K.J. van Duren, P.A. van Hal, J.L.J. van Dongen, R.A.J Janssen, Synthesis and characterization of a low bandgap conjugated polymer for bulk heterojunction photovoltaic cells, Advanced Functional Materials 4 (11) (2004) 255–262.
[51] D. Mühlbacher, M. Scharber, M. Morana, Z. Zhu, D. Waller, R. Gaudiana, C. Brabec, High photovoltaic performance of a low-bandgap polymer, Advanced Materials 18 (2006) 2884–2889.
[52] C. Brabec, C. Winder, N.S. Sariciftci, J.C. Hummelen, A. Dhanabalan, P.A. van Hal, R.A.J. Janssen, A low-bandgap semiconduction polymer for photovoltaic devices and infrafed emitting diodes, Advanced Functional Materials 10 (12) (2002) 709–712.
[53] M.K.R.J. Velusamy, J.T. Thomas, Y.-C. Lin, K.-C. Hsu, Ho, Organic dyes incorporating low-band-gap chromophores for dye-sensitized solar cells, Organic Letters 7 (10) (2005) 1899–1902.
[54] E. Bundgaard, F.C. Krebs, Low band gap polymers for organic photovoltaics, Solar Energy Materials and Solar Cells 91 (2007) 954–985.
[55] L.J.A. Koster, V.D. Mihailetchi, P.W.M Blom, Ultimate efficiency of polymer/fullerene bulk heterojunction solar cells, Applied Physics Letters 88 (2006) 093511.
[56] J. Zhao, A. Wang, P. Campbell, M.A. Green, A 19.8% efficiency honeycomb multicrystalline silicon solar cell with improved light trapping, IEEE Transactions on Electron Devices 46 (10) (1999) 1978–1983.
[57] J. Zhao, P. Wang, M.A. Green, F. Ferrazza, 19.8% efficiency honeycomb textured multicrystalline and 24.4% monocrystalline silicon solar cells, Applied Physics Letters 73 (1998) 1991.
[58] N. Koide, R. Yamanaka, H. Katayama, Recent advances of dye-sensitized solar cells and integrated modules at Sharp, Materials Research Society Symposium Proceedings 1211 (2010).
[59] M.A. Green, K. Emergy, Y. Hishikawa, W. Warta, E.D. Dunlop, Solar cell efficiency tables (version 39), Progress in Photovoltaics: Research and Applications 20 (2012) 12–20.